MODELING OF AERODYNAMICS IN VORTEX FURNACE

I.S. Anufriev*, V.V. Salomatov*,, Y.A. Anikin*,**, D.V. Krasinsky*, O.V. Sharypov*,****

anufriev@itp.nsc.ru

*Kutateladze Institute of Thermophysics, Siberian Branch, Russian Academy of Sciences, Novosibirsk, Russia

**Novosibirsk State University, Novosibirsk, Russia

Abstract

At present, the torch burning technology of pulverized-coal fuel in vortex flow is one of the most prospective and environmentally-friendly combustion technologies of low-grade coals. Appropriate organization of aerodynamics may influence stability of temperature and heat flux distributions, increase slag catching, and reduce toxic emissions. Therefore, from scientific point of view it is interesting to investigate aerodynamics in the devices aiming at justification of design and operating parameters for new steam generators with vortex furnace, and upgrade of existing boiler equipment. The present work is devoted to physical and mathematical modeling of interior aerodynamics of vortex furnace of steam generator of thermal power plants.

Research was carried out on the air isothermal model which geometry was similar to one section of the experimental-industrial boiler TPE-427 of Novosibirsk TPS-3. Main elements of vortex furnace structure are combustion chamber, diffuser, and cooling chamber. The model is made from organic glass; on the front wall two rectangular nozzles (through which compressed air is injected) are placed symmetrically at 15º to the horizon. The Laser Doppler Velocimeter LAD-05 was used for non-contact measurement of vortex flow characteristics. Two velocity components in the XY-plane (in different cross-sections of the model) were measured in these experiments. Reynolds number was $3 \cdot 10^5$.

Numerical simulation of 3-D turbulent isothermal flow was performed with the use of CFD package FLUENT. Detailed structure of the flow in vortex furnace model has been obtained in predictions. The distributions of main flow characteristics (pressure, velocity and vorticity fields, turbulent kinetic energy) are presented.

The obtained results may be used at designing boilers with vortex furnace. Computations were performed using the supercomputer NKS-160. The work was supported by RFBR (projects No. 10-08-01093-a, 10-08-90032-Bel_a) and Russian Ministry of Education and Science (ADTP “Development of scientific potential of higher school” and FTP “Research and Pedagogical Cadre for Innovative Russia”, “Research and Development in Priority Directions of Development of Scientific-Technological Complex of Russia”).

Introduction

One of the perspective and environmentally-friendly combustion technologies of low-grade coals is torch burning of pulverized-coal fuel in vortex flow [1]. It is important to point out that vortex transfer appears to be the aerodynamic basis of the entire combustion process. Aerodynamic structure of swirl flow in vortex furnaces generates stable energy-intensive high-turbulent circulation zones playing determinant role in acceleration of the slowest processes of gasification and mixing. Optimal organization of aerodynamics may influence intensity of fuel burnout, provide necessary level of volumetric and surface heat intensities, satisfy rather strict requirements to distribution of velocities, concentrations, temperature and heat fluxes, increase slag catching at liquid slag disposal, decrease toxic emissions, etc.

Furnace processes are significantly influenced by such aerodynamic phenomena of the vortex flow as attachment of a torch with one of the heated surfaces (Coanda effect), precession of vortex core, secondary flows and recirculation zones. So, the first effect caused by ejection may result in torch deviation from initial direction to the wall; this results in the separation of coal particles and oxidizer and increases mechanical underburning, besides it results in thermally intense working conditions of furnace screens in places of torch-wall contact. Flow curvature leads to particles separation from the torch, and hence intense slagging of screen surfaces. The second and third effects foster active mixing of fuel and oxidizer, accelerate warming-up of the pulverized-coal jet supplied to combustion chamber for the account of intersection of cold fuel mixture at the inlet with hot torch combustion products. Presence of the large-scale reverse flows in the furnace space results in reduction of the flow-through part cross-sections, appearance of stagnation zones where due to ejection effect the induced circulation vortices of combustion products or excessive air move. On the other hand this fosters afterburning of fuel particles in reverse flows due to the increased time of their presence in the furnace volume. This is far from being a complete list of both positive and negative factors of aerodynamics influence on the furnace process (and hence on reliability and economic efficiency of steam generator); it proves topicality of investigation of aerodynamic of swirl flow characteristics aiming at substantiation of design and operating parameters of new steam generators with vortex furnaces as well as modernization of existing boiler equipment.

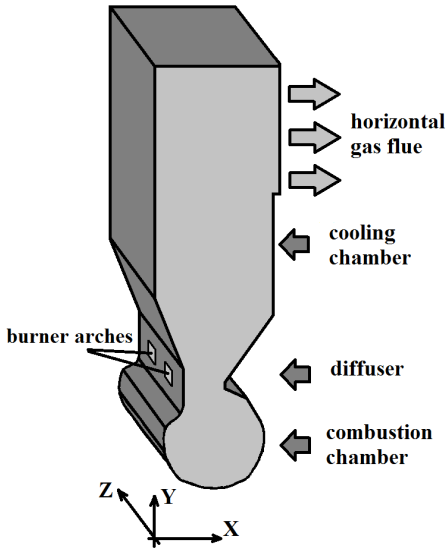

Figure 1. Scheme of a vortex furnace.

The vortex furnace of the experimental-industrial boiler TPE-427 designed by N.V. Golovanov (JSC CBTI) of Novosibirsk HPP-3 has been investigated at the present work (Fig. 1). Principle elements of the vortex furnace are combustion chamber where main combustion of tangentially injected pulverized coal takes place, diffuser and cooling chamber ending with horizontal gas flue. Advantages of the design are rational mass-dimensional characteristics of a furnace, single-frontal positioning of the burners and maneuverability characteristics. Combustion occurs at increased volumetric heat intensity providing free-flowing liquid state of slag. In such furnaces intense assimilation of fused ash particles by lining slag layer increases slag catching coefficient in the furnace and decreases flue ash removal.

Analysis of fundamental works related to the vortex furnace of this type performed earlier by CBTI researchers, authors of this work from IT SB RAS and other scientists still proves insufficient knowledge on the complex structure of swirl flows especially on three-dimensional effects. This prevents further modernization of existing and development of new perspective boiler units with vortex burning technology on a modern scientific basis. Compared with the methods of investigation applied earlier today we witness the progress in the development of precision measurement systems in particular laser-Doppler diagnostics. Besides, reputable Commercial codes for instance, FLUENT, are now available for the users. At this stage they provide an opportunity to receive detailed (earlier inaccessible) information on the parameters of turbulent swirl flow practically in any point of a furnace chamber. Therefore the objective of this work is to further experimental and theoretical study of aerodynamic characteristics of swirl flows, and as a first step to carry out investigation in isothermal model of vortex furnace of power steam generator.

Experimental setup and measurement method

Physical modeling of internal aerodynamics of the studied vortex furnace was carried out in the isothermal model with the geometry (in a scale 1:15) similar to one of the sections of the experimental-industrial boiler TPE-427 of Novosibirsk HPP-3 (Fig. 2). The model was manufactured from organic glass with specific dimensions: x_{max}= 300 mm, y_{max}= 1300 mm, z_{max}= 330 mm, relation of the diffuser neck width to the diameter of vortex combustion chamber is H_x = 0.24. On the front wall at 15º angle to horizon there are two rectangular nozzles (that agree with burner arches), through which compressed air is supplied [2].

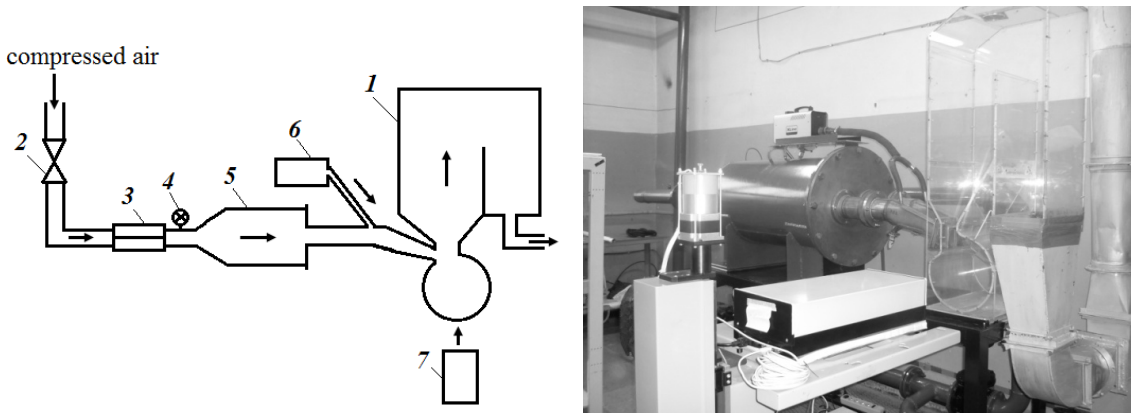

Figure 2. Experimental setup for investigation of aerodynamics and mixing processes in vortex furnace: 1 – model of vortex furnace; 2 – valve; 3 – pressure regulator (reducer); 4 – manometer; 5 – receiver (for pressure pulsations smoothing); 6 – smoke generator XLINE FOG 800; 7 – automated measurement complex LAD-05.

At physical modeling we used geometry parameter of similarity Σ_f/F_T, specific for this type of steam generators with vortex furnace, where Σ_f is sum of burner section areas, F_T – area of diametral cross-section of combustion chamber. Reynolds number (Re~10^5) at laboratory conditions is lower than at the natural ones. Modeling of flow structure at that is justified due to the flow self-similarity in the range of Re = $10^4 \div 10^6$ [3].

Experimental methodology was as follows (see Fig. 2). Compressed air flow was supplied from the line to the model of vortex furnace (1) through pressure regulator (3) and receiver (5) to stabilize flow rate. Pressure after the regulator was controlled with the use of manometer (4). For non-contact measurement of steady-state distribution of flow velocity in the model sections of interest laser-Doppler precision measurement system (automated Laser Doppler

Velocimeter LAD-05), developed in IT SB RAS was used [4]. The system includes: optoelectronic module, coordinate-shifting device (CSD), and computer with specialized software. In optoelectronic module optical scheme with backward scattering is realized; its advantage is usage of semiconductor laser. The laser beam is split by acousto-optic modulator into two beams. The beams, intersecting in the flow, form interferential field with the known periodic structure. Its image in the backward scattered light is formed by optical elements on the light-sensitive surface of photoreceiver. The method is based on measuring shifts of particles suspended in the flow (tracers). Crossing interferential field particles generate optical signal which frequency is directly proportional to the tracers' velocity. In the experiment microdrops of special liquid (based on glycerin) produced by smoke generator were used as tracers. Tracers were admixed to main air flow through the nozzles' holes before the inlet to the model and so filled the entire studied volume. Their concentration allowed the measurement system to register 300–500 particles per second. Specific size of microdrops (1–5·mcm) provided high correspondence of their trajectories to stream lines.

Automated measurement complex LAD-05 measures two components of the flow velocity lying in the plane perpendicular to the optical axis of optoelectronic block. The system was located so that the optical axis to coincide with the axis of cylindrical part of the furnace model. Thus the measured velocity components were in the plane *XY* (the plane perpendicular to the axis *z*), further they are designated as *U* and *V* (projections to the axes *x* and *y*, respectively). CSD moves optoelectronic block along three axes that serves to position the measurement volume of the system in any point inside the furnace model. Minimal step of a shift was 0.01 mm, positioning accuracy was limited by the accuracy of referencing to coordinate origin and was not worth than 1 mm. The range of CSD shifts over each axis was limited by the value 250 mm. The dimensions of the studied area of the furnace model were 300x500x200 mm. To measure the whole area of interest it was required to carry out several series of measurements and combine results taking into account coordinate unification in one reference system. Two flow velocity components were measured in the planes *XY* (at different values of coordinate *z*) in the grid nodes 28×47 with spatial step of 1 cm.

Main contribution in the error of average value measurement is made by velocity pulsations. Since average velocities in different points substantially differ it is expedient to give the size of the confidence interval in relative values reduced to average velocity in the given point:

$$U = \bar{U} \pm \Delta U = \bar{U}\left(1 \pm \frac{t(\alpha, N)S}{\bar{U}\sqrt{N}}\right),$$

where S is calculated standard deviation, N – number of measurements in the point, α – probability of entry in the confidence interval, $t(\alpha, N)$ – Student's quantile. Automated experiment was planned for no less than 1000 measurements in every experiment point ($N = 500$ for each velocity component) to result in the average velocity value. For $\alpha = 0.95\%$ and $N > 25$, $t(\alpha, N) \approx 2$. It has been found out that for each point of experiment relation of standard deviation to the average value did not exceed $\frac{S}{\bar{U}} < 0,35$. Then $\frac{t(\alpha, N)S}{\bar{U}\sqrt{N}} < 0,035$. I.e. for each measurement point 95% confidence interval did not exceed 3.5% of the calculated local average velocity. Velocity pulsations determined as mean square deviation of all measurements in the point did not exceed 1.2 m/s in each point of experiment.

Numerical simulation

Flow in the vortex furnace is subsonic and turbulent and has essentially spatial character conditioned by structural scheme of the furnace. Numerical simulation of such flow in isothermal three-dimensional statement was carried out with the use of CFD-packet FLUENT ver.6.3. Mathematical model of the steady-state spatial turbulent flow is based on continuity and momentum equations averaged on Reynolds; for their closing the so called "realizable" modification of k-ε turbulence model was used [5]. The advantage of this model compared with the "standard" k-ε turbulence model [6] is the lesser number of constants (so, the values of the parameter C_μ are determined as a function of k, ε and velocity gradients and better agree with experimental observations than assumption $C_\mu = \text{const}$ in "standard" k-ε model). Besides its merits are more accurate formulation of the terms in the equation of turbulence transfer of dissipation velocity ε (deduced in [5] from exact equation for the transfer of the second moment of vorticity pulsations) providing much better predictive potential of the model (for example: adequate calculation of axis-symmetrical jet propagation velocity, applicability for swirl flow simulation and/or flows with significant stream line curvature, etc.) and its improved calculation robustness. In this model it is sufficient to preset only four constants: $C_{1\varepsilon} = 1.44$; $C_2 = 1.9$; $\sigma_k = 1$; $\sigma_\varepsilon = 1.2$.

The studied option of the vortex furnace design has a symmetry plane S_{XY} (in the section $z = 165$ mm) between two burners positioned in series in the direction to axis z (see Fig. 1). The flow is assumed symmetrical in relation to this plane, therefore to save computing resources only half of the furnace volume was calculated. The unstructured computational grid built for finite-volume discretization of equations consists of 254848 hexahedral cells; its view on the boundary surface of the simulated furnace volume is given in the Fig. 3 (for more vivid presentation only the area of vortex chamber and furnace diffuser are shown). The average grid step inside the vortex chamber is approximately 6 mm, at that close to the chamber walls the grid is thickened so that the distance along normal from the wall to the center of the first cell is about 0.9 mm. In the upper part of the furnace the average grid step is from 8 to 15 mm, at that close to the chamber walls the grid is thickened so that the distance along normal from the wall to the center of the first cell is from 1.5 to 2 mm.

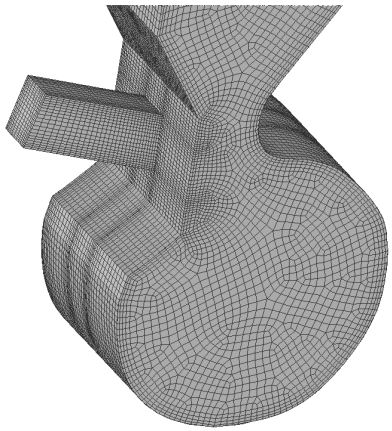

Figure 3. The view of the computational grid on the surface of the swirl furnace.

For velocity components on the walls the sticking boundary conditions are set, at that to simulate turbulence in the wall area we use the method of "improved near-wall simulation" [7, 8] being a combination of two-zone description (with separation of a viscous sublayer zone and buffer zone when turbulent number $\text{Re}_r < 200$, r – distance along normal from the wall to the center of the near-wall cell) with description according to the modified method of

the near-wall functions [9], including consideration of pressure gradient and non-equilibrium effects caused by current lines curvature in a complex spatial boundary layer. Such combined methodology [8] serves to more accurate consideration of the influence of viscous sublayer and buffer zone without the necessity to significantly reduce the grid (along normal to the wall) in these zones. For the used grids values of dimensionless distance to the wall in the near-wall cells turn out to be in the range $10 < r < 100$.

As boundary conditions in the second section of rectangular nozzle channel we set even profile of average flow rate equal on the module to U_0=15 m/s. Turbulence parameters k_0 and ε_0 in this section were determined by the value of turbulent pulsations intensity assumed equal to 5%. On the plane S_{XY} conditions of mirror symmetry for all values are set. Canal of the rotary (exhaust) air flue of the boiler has sufficient extension from top to bottom (~1 m, i.e. approx. 5 calibers in relation to air flue width, see Fig. 1), to obtain flow characteristics close to the uniform ones – in this section for all values apart from pressure the so called "soft" boundary conditions are set, and pressure gradient in the outlet section is determined from integral condition of mass balance conservation.

For numerical approximation of convective members of the averaged momentum equations we used the scheme QUICK [10] with improved accuracy order; and for turbulent transfer equations – Patankar scheme of "the fifth degree" [11] providing solution monotony for scalar quantities. To disintegrate nonlinear relation between velocity and pressure components the algorithm PISO was used [12]. This algorithm is a modification of the known SIMPLE [11] with additional internal iterations introduced for velocity and pressure correction of "predictor-corrector" type reduced to solution of additional number of Poisson equations for pressure corrections. Despite the increase of the calculation scope in each "global" iteration additional "sub-iterations" of "predictor-corrector" in PISO algorithm provide much better agreement of velocity and pressure fields resulting in more reliable and fast convergence of iteration process as a whole.

Results of investigations and their analysis

Experimental data and numerical calculations were obtained at the same starting conditions: the working medium – compressed air; Reynolds number calculated on the basis of the vortex furnace diameter (0.29 m) was $\mathrm{Re} = 3 \cdot 10^5$ (at that average flow rate on the nozzle section was U_0=15 m/s, air density at the temperature of 20 °C $\rho_0 = 1.2$ kg/m^3, dynamic viscosity of air at the temperature 20 °C $\mu_0 = 1.82 \cdot 10^{-5}$ Pa·s). The nozzle size in the section at the combustion chamber inlet was 40×60 mm.

Flow structure in the model of the vortex furnace is shown in the Figs. 4, 5. In the Fig. 4 there is flow velocity projection distribution on the plane XY at $z = 0.23$ (section over the nozzle center, 75 mm from the end wall of the model), and in the Fig. 5 – at $z = 0.5$ (section in the middle of the nozzles, 165 mm from the end walls of the model). From the analysis of results presented in the Fig. 4 and 5, it may be inferred that the swirl flow in combustion chamber has spatial structure where vortex center position does not depend on the coordinate z. Both computational and experimental data (see Fig. 5) demonstrate significant spatial heterogeneity of the ascending flow in the cooling chamber. The flow goes out through combustion chamber diffuser as a jet between the nozzles; it sticks to the walls of the cooling chamber (Coanda effect). This phenomenon in practice may lead to negative results. It is conditioned by the vortex furnace design, in particular by low relative value of the neck width of combustion chamber diffuser ($H_x = 0.24$) and its close position to the frontal wall of cooling chamber that fosters demonstration of Coanda effect.

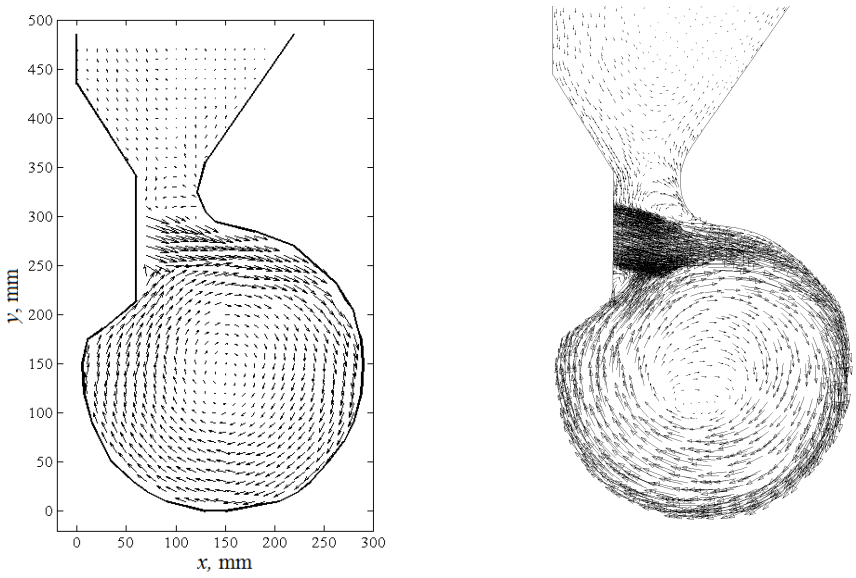

a) *b*)

Figure 4. Velocity field in vortex furnace model at $z = 0.23$ (section XY over the nozzle center): experimental data (*a*), results of numerical simulation (*b*).

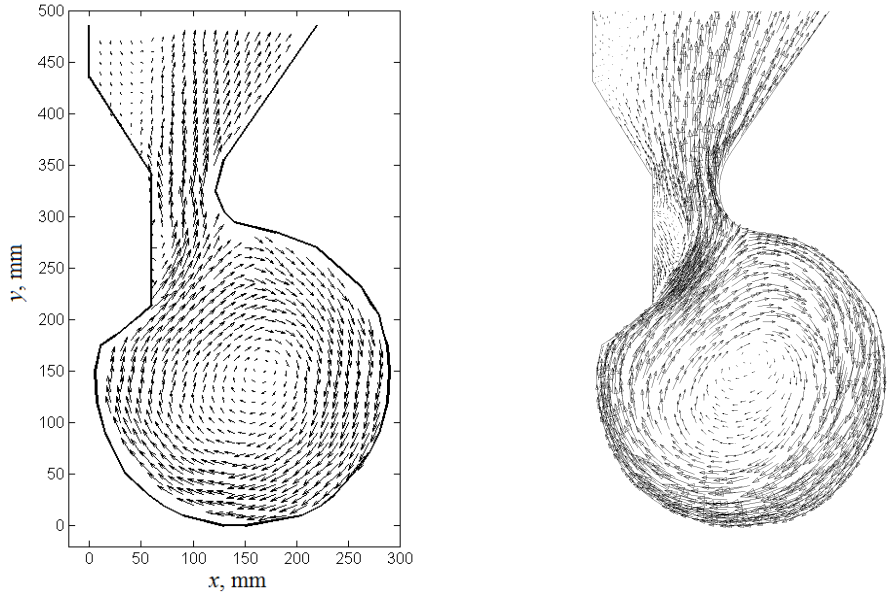

a) *b*)

Figure 5. Velocity field in vortex furnace model at $z = 0.5$ (section XY between the nozzles): experimental data (*a*), results of numerical simulation (*b*).

In the Figs. 6–11 there are field distributions of U, V velocity components and velocity module in the sections over the nozzle center ($z = 0.23$) and in the middle of the nozzles ($z = 0.5$). It is apparent that experimental data and results of numerical calculations fairly agree. Besides, results presented in the Figs. 10-11 also demonstrate spatial flow structure in vortex furnace model.

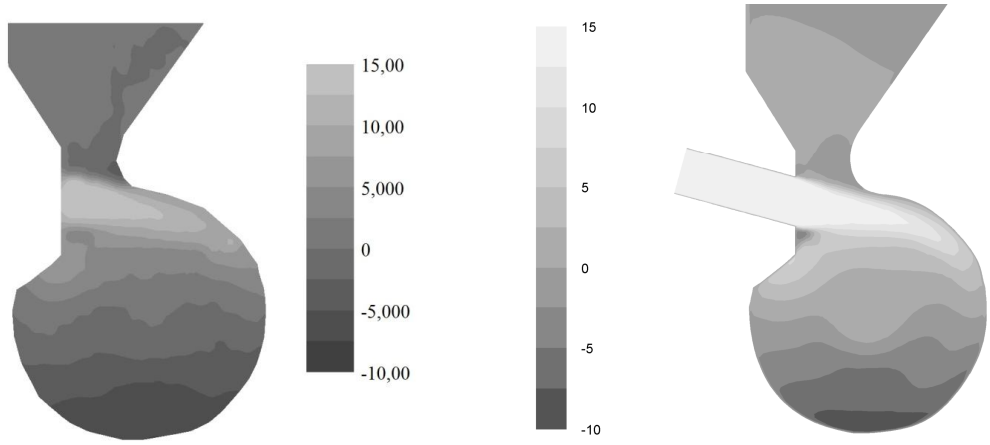

a) *b*)

Figure 6. Distribution of *U*-velocity component (m/s) inside the studied model of the vortex furnace (section $z = 0.23$): results of LDA-measurements (*a*); numerical calculations (*b*).

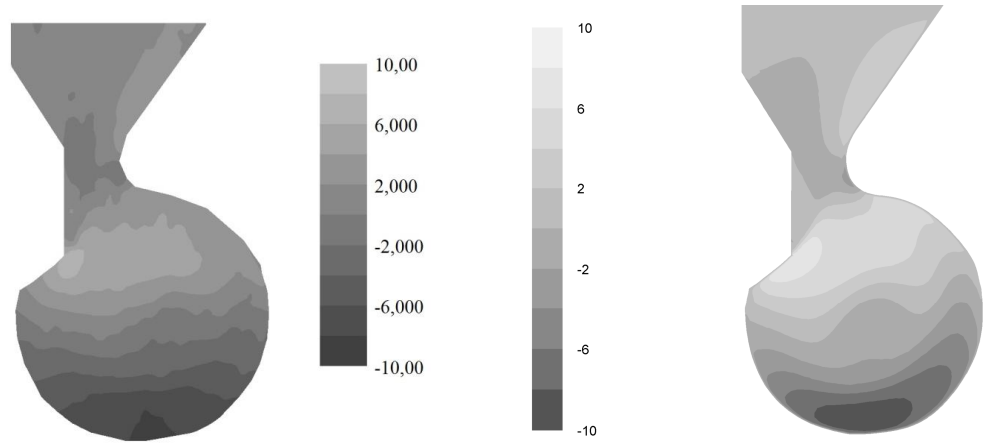

a) *b*)

Figure 7. Distribution of *U*-velocity component (m/s) inside the studied model of vortex furnace (section $z = 0.5$): results of LDA-measurements (*a*); numerical calculations (*b*).

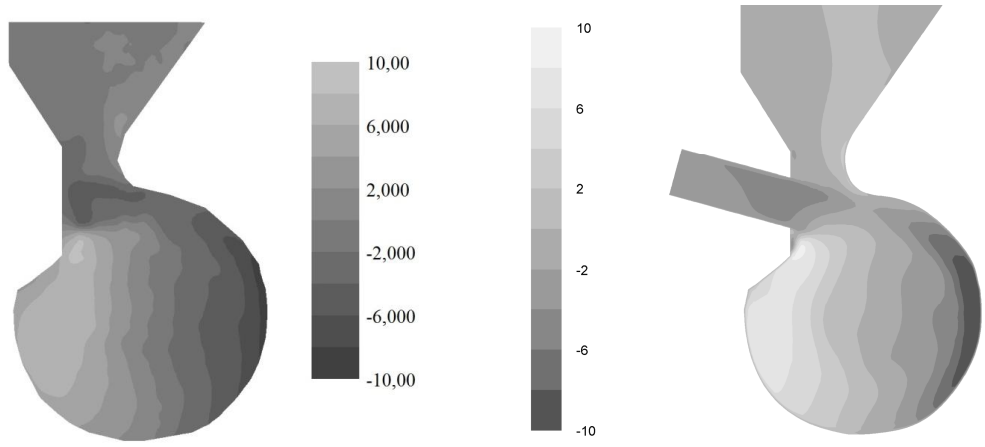

a) *b*)

Figure 8. Distribution of *V*-velocity component (m/s) inside the studied model of vortex furnace (section $z = 0.23$): results of LDA-measurements (*a*); numerical calculations (*b*).

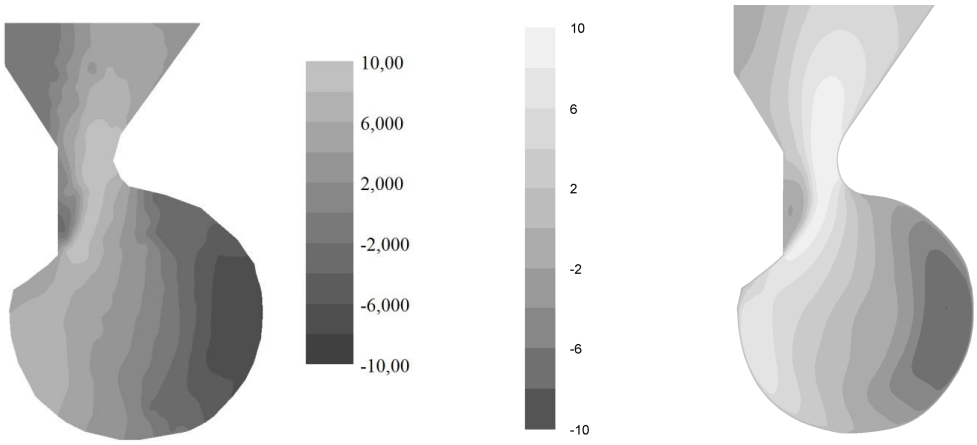

a) *b*)

Figure 9. Distribution of *V*-velocity components (m/s) inside the studied model of vortex furnace (section $z = 0.5$): results of LDA-measurements (*a*); numerical calculations (*b*).

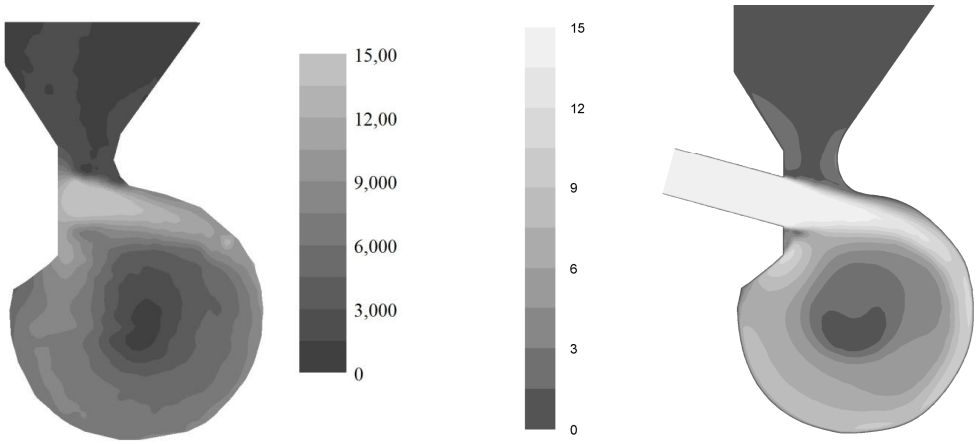

a) *b*)

Figure 10. Distribution of velocity module (m/s) inside the studied model of vortex furnace (section $z = 0.23$): results of LDA-measurements (*a*); numerical calculations (*b*).

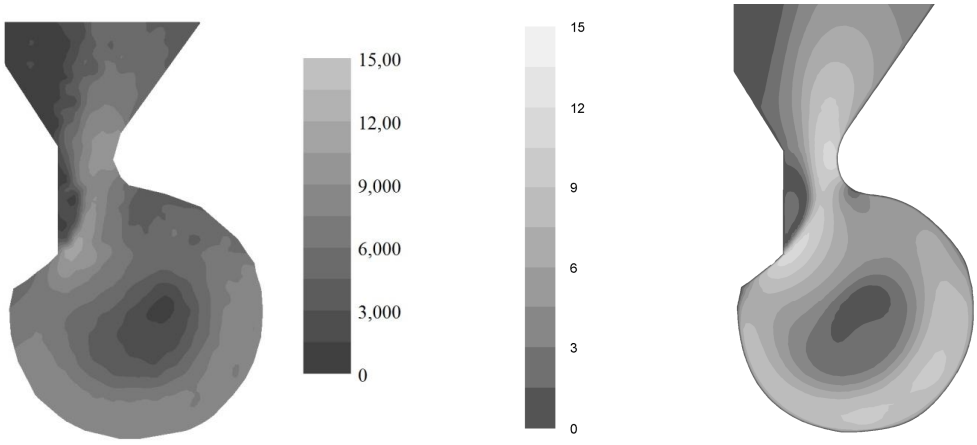

a) *b*)

Figure 11. Distribution of velocity module (m/s) inside the studied model of vortex furnace (section $z = 0.5$): results of LDA-measurements (*a*); numerical calculations (*b*).

In the Figs. 12-16 there are distributions of main aerodynamic characteristics of isothermal flow in the studied model of vortex furnace (vertical and horizontal velocity

components, turbulent kinetic energy) along the horizontal line passing through combustion chamber center (y = 150 mm), and along the vertical line passing through the center of diffuser neck (x = 93.5 mm), in two sections (over the nozzle center and between the nozzles). Here results of numerical calculations and data of LDA-measurements are presented. In the Fig. 12 there are also data of hot-wire anemometer measurements [13].

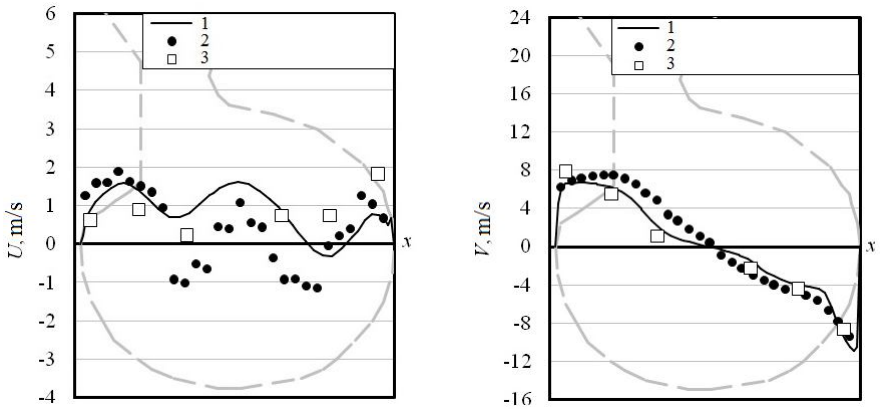

a) *b*)

Figure 12. Distribution of horizontal U (*a*) and vertical V (*b*) velocity components along the horizontal line passing through combustion chamber center (y = 150 mm), in the section z = 0.23 (1 – numerical calculations; 2 – results of LDA-measurements; 3 – hot-wire anemometer measurements).

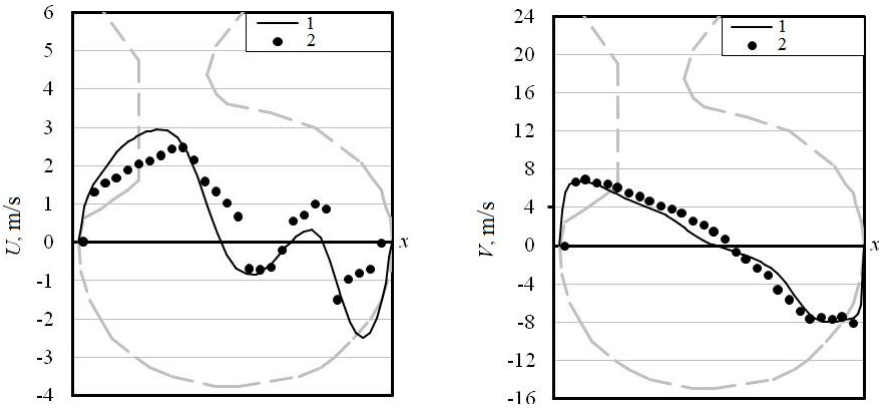

a) *b*)

Figure 13. Distribution of horizontal U (*a*) and vertical V (*b*) velocity components along the horizontal line passing through combustion chamber center (y = 150 mm), in the section z = 0.5 (1 – numerical calculations; 2 – results of LDA-measurements).

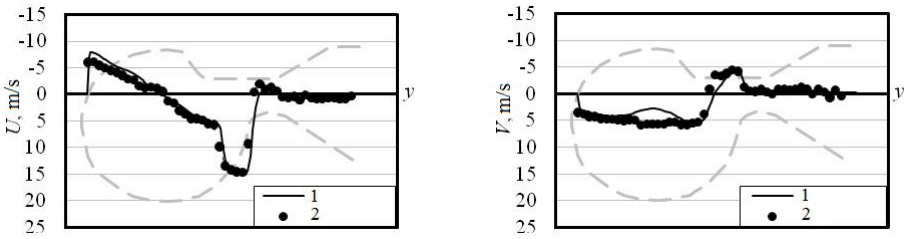

a) *b*)

Figure 14. Distribution of horizontal U (*a*) and vertical V (*b*) components along the vertical line passing through the diffuser neck center (x = 93.5 mm), in the section z = 0.23 (1 – numerical calculations; 2 – results of LDA-measurements).

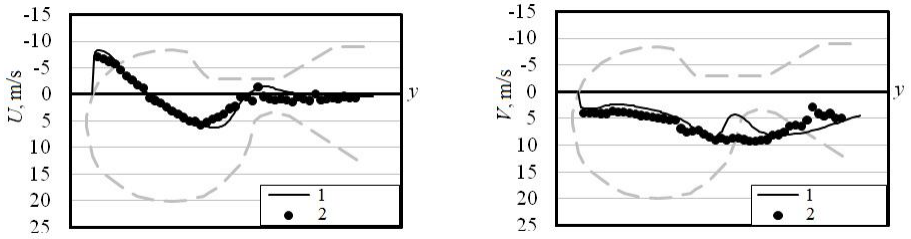

a) *b*)

Figure 15. Distribution of horizontal U (*a*) and vertical V (*b*) velocity components along the vertical line passing through the center of diffuser neck (x = 93.5 mm), in the section z = 0.5 (1 – numerical calculations; 2 – results of LDA-measurements).

From the Fig. 13-*a* it is apparent that horizontal velocity component changes sign three times. Negative values in the right part of the graph may be explained by the fact that incoming jet in this section continues even distribution in horizontal direction. Analysis of the Figs.12-*b*, 13-*b* shows that profile of vertical velocity component in the vortex combustion chamber is stable and close to axisymmetrical, besides it agrees with velocity distribution in the flow with potential vortex. Insignificant deviation is observed in the center of the vortex since due to intense turbulent mixing there is the overbending area with practically zero vertical component. The flow in the diffuser part has a "glove" character, carrying-out occurs in the symmetry plane between two arches. Profiles of vertical and horizontal velocity components presented in the Figs. 14-15, demonstrate motion in axial direction that proves once again essentially three-dimensional character of vortex furnace aerodynamics.

Processing of LDA-measurement results allows obtaining distribution of kinetic energy of flow turbulence determined with the formula $k_t = 0,5\left(\overline{(U')^2 + (V')^2}\right)$, where U', V' are deviations from the average value of horizontal and vertical velocity components respectively, and the line on top is an averaging symbol. In the Fig. 16 there are distributions of kinetic energy of turbulence over the horizontal line passing through the center of combustion chamber, in the section at the nozzle center and in the section between the nozzles. From the Fig. 16 it is apparent that profiles of kinetic energy of turbulence have maximum value at the right wall of the model that is apparently caused by "washing-out" of the incoming jet developing the flow swirl. Intensity of kinetic energy of turbulence decreases toward the left wall. Such fast laminarization of the flow is caused by centrifugal force arising at the flow along the concave wall.

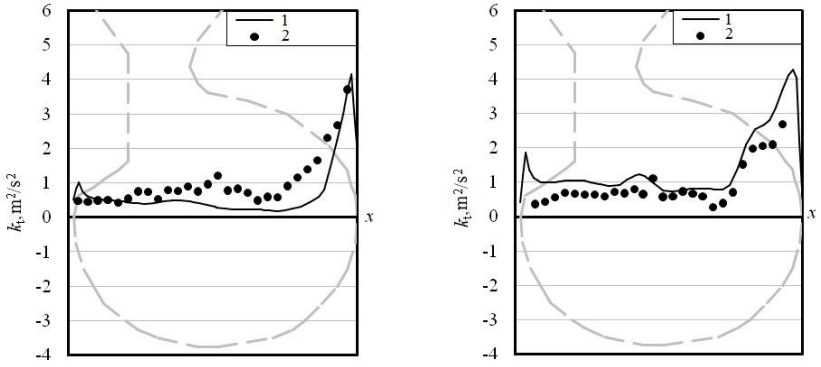

a) *b*)

Figure 16. Distribution of kinetic energy of turbulence along the horizontal line passing through the center of combustion chamber (y = 150 mm): section z = 0.23 (*a*); section z = 0.5 (*b*) (1 – numerical calculations; 2 – results of LDA-measurements).

Conclusion

With the use of non-contact LDA method and numerical simulation internal aerodynamics of laboratory model of the vortex furnace of the experimental-industrial boiler TPE-427 has been investigated. The measured and calculated fields of velocity components and respective pulsation components serve to come to the following conclusions. The swirl flow in combustion chamber of the model has spatial structure for which position of the vortex center does not depend on the coordinate *z*. The flow in diffuser part has a "glove" character, carry-out occurs in the symmetry plane between two burner arches. At the flow outlet from the vortex zone its fast laminarization takes place. Coanda effect – "sticking" of the jet to the cooling chamber wall at diffuser outlet – takes place. Its rise is conditioned by low relative value of diffuser neck width and its close positioning to the frontal wall of the cooling chamber. Close to the frontal wall of the model there is reverse flow area that is bound with slightly incorrect positioning of the burners according to their heights. Over the transverse section of a cooling chamber there are both vertical and horizontal vortices.

The mentioned peculiarities of the turbulent flow aerodynamics in the vortex furnace shall be considered at designing new furnaces of this type and boilers reconstruction and reconfiguration to the mode of vortex combustion with improved characteristics.

References

[1] Salomatov, V.V., *Environmental technologies at heat and nuclear power plants*, Novosibirsk, 2006, p. 853. (in Russian)

[2] Salomatov, V.V., Sharypov, O.V., Anufriev, I.S., Anikin, Yu.A., Enkhjargal, Kh., "Physical modeling of interior aerodynamics of energy steam generator vortex furnace", *Vestnik NGU. Ser: Fizika.* Vol. 6 (1): 60-65 (2011). (in Russian)

[3] Kutateladze, S.S., *Similarity analysis in thermophysics*, Novosibirsk, 1982, p. 280.

[4] Meledin, V.G., Anikin, Yu.A., Bakanin, G.V., et al., "Laser Doppler Velocimeter LAD-05 for 2-D diagnostics of liquid-gas flow", *Proc Conference on High Technologies, Fundamental and Applied Research, Education*, St.Petersburg, Russia, 2006, Vol.5, pp. 343-344.

[5] Shih, T.-H., Liou, W.W., Shabbir, A., Yang, Z., Zhu, J.A, "New k-ε Eddy-Viscosity Model for High Reynolds Number Turbulent Flows – Model Development and Validation", *Computers & Fluids*, Vol. 24 (3): 227-238 (1995).

[6] Launder, B.E., Spalding, D.B., *Lectures in Mathematical Models of Turbulence*, London (England): Academic Press, 1972.

[7] Jongen, T., *Simulation and Modeling of Turbulent Incompressible Flows*, PhD thesis, Lausanne (Switzerland): EPF Lausanne, 1992.

[8] FLUENT 6.3 User's Guide // *Fluent Inc.*, 2006.

[9] Kim, S.-E., Choudhury, D.A., "Near-Wall Treatment Using Wall Functions Sensitized to Pressure Gradient", *In ASME FED Vol. 217, Separated and Complex Flows.*, ASME, 1995.

[10] Leonard, B.P., Mokhtari, S., "ULTRA-SHARP Nonoscillatory Convection Schemes for High-Speed Steady Multidimensional Flow", *NASA TM 1-2568 (ICOMP-90-12)*, NASA Lewis Research Center, 1990.

[11] Patankar, S. *Numerical heat transfer and fluid flow*, Hemisphere Publishing Corporation, New York, 1980.

[12] Issa, R.I., "Solution of Implicitly Discretized Fluid Flow Equations by Operator Splitting", *J. Comput. Phys.*, Vol. 62: 40-65 (1986).

[13] Keyno, A.W., Krasinsky, D.V., Rychkov, A.D., Salomatov, V.V., "Experimental and numerical modeling of the vortex furnace aerodynamics", *Russ. J. Eng. Thermophys.*, Vol. 6: 47-62 (1996).